A&A 421, 899–911 (2004)
DOI: 10.1051/0004-6361:20035676

Astronomy & Astrophysics

A new sample of large angular size radio galaxies

III. Statistics and evolution of the grown population

L. Lara[1,2], G. Giovannini[3,4], W. D. Cotton[5], L. Feretti[3], J. M. Marcaide[6], I. Márquez[2], and T. Venturi[3]

[1] Dpto. Física Teórica y del Cosmos, Universidad de Granada, Avda. Fuentenueva s/n, 18071 Granada, Spain
[2] Instituto de Astrofísica de Andalucía (CSIC), Apdo. 3004, 18080 Granada, Spain
[3] Istituto di Radioastronomia (CNR), via P. Gobetti 101, 40129 Bologna, Italy
[4] Dipartamento di Astronomia, Universitá di Bologna, via Ranzani 1, 40127 Bologna, Italy
[5] National Radio Astronomy Observatory, 520 Edgemont Road, Charlottesville, VA 22903-2475, USA
[6] Departimento de Astronomía, Universitat de València, 46100 Burjassot, Spain

Received 13 November 2003 / Accepted 3 April 2004

Abstract. We present in this paper a detailed study of a new sample of large angular size FR I and FR II radio galaxies and compare the properties of the two classes. As expected, a pure morphology based distinction of FR Is and FR IIs corresponds to a break in total radio power. The radio cores in FR Is are also weaker than in FR IIs, although there is not a well defined break power. We find that asymmetry in the structure of the sample members must be the consequence of anisotropies in the medium where the lobes expand, with orientation playing a minor role. Moreover, literature data and our observations at kiloparsec scales suggest that the large differences between the structures of FR I and FR II radio galaxies must arise from the poorly known central kiloparsec region of their host galaxies. We analyze the sub-sample of giant radio galaxies, and do not find evidence that these large objects require higher core powers. Our results are consistent with giant radio galaxies being the older population of normal FR I and FR II objects evolving in low density environments. Comparing results from our sample with predictions from the radio luminosity function we find no evidence of a possible FR II to FR I evolution. Moreover, we conclude that at $z \sim 0.1$, one out of four FR II radio sources has a linear size above 500 kpc, thus being in an advanced stage of evolution (for example, older than ∼10 Myr assuming a jet-head velocity of 0.1c). Radio activity seems to be a short-lived process in active galaxies, although in some cases recurrent: five objects in our sample present signs of reactivation in their radio structures.

Key words. galaxies: active – galaxies: nuclei – galaxies: jets – radio continuum: galaxies

1. Introduction

Radio galaxies, with linear sizes reaching up to several megaparsecs, are possibly the largest individual objects in the Universe. It is widely accepted that they originate from highly energetic non-thermal processes occurring in the nucleus of the so-called active galaxies (Blandford & Rees 1974; Rees 1978). According to the standard model of active galactic nuclei (AGNs), a super-massive black hole with a mass between 10^6 and 10^9 $M_\odot$, resides in the center of the active galaxy, powered by an accretion disk surrounded by a torus formed by gas and dust. In about 10% of these AGNs, there is intense synchrotron radio emission produced in a bipolar outflow of relativistic particles expelled perpendicularly to the plane of the disk and extending to distances reaching the megaparsec scales. The reason why an AGN presents or not powerful radio emission is matter of strong debate. While there is increasing evidence about the existence of super-massive black holes in the center of AGNs, and even at the nuclei of non active galaxies (Macchetto 1999; Kormendy & Gebhardt 2001), it has been argued that the presence or not of intense radio emission might be due to the rotation velocity of the black hole (e.g., Wilson & Colbert 1995; Cavaliere & D'Elia 2002), or to its total mass and the efficiency of accretion (McLure & Dunlop 2001; Dunlop et al. 2003).

Considering a natural evolutionary sequence of radio galaxies, jets emanating from the center of activity start boring their way through the interstellar medium first, reaching the galactic halo and in some large cases the intergalactic medium. Finally, the lobes of radio galaxies which have ceased their central activity expand and disappear in the external medium. Radio sources representing these different phases of evolution are currently known adding support to this scenario: compact symmetric objects (CSOs; Wilkinson et al. 1994) are thought to be young radio galaxies (e.g., Owsianik & Conway 1998), while the giant radio galaxies (GRGs; defined as those with a projected linear size[1] ≥1 Mpc) are probably old objects at the

Send offprint requests to: L. Lara, e-mail: lucas@ugr.es

[1] We assume that $H_0 = 50$ km s^{-1} Mpc^{-1} and $q_0 = 0.5$.

latter stages of evolution (Ishwara-Chandra & Saikia 1999). Relic radio sources found in clusters of galaxies might correspond to the last detectable emission from "dead" radio galaxies (e.g., Komissarov & Gubanov 1994; Slee et al. 2001).

However, the degree of influence of parameters other than the age (e.g. source power, conditions of the external medium) in the evolution of radio galaxies is not clear . For example, although there is observational evidence supporting the young source scenario for CSOs, it has also been argued that CSOs are short lived objects which never reach the size of their big relatives (Readhead et al. 1994). At the other extreme, GRGs could be the result of normal radio galaxies expanding in very low density environments permitting them to reach their overwhelming sizes. But they could also result from very powerful core activity, or both conditions must apply for a radio galaxy to become a giant. Complicating the previously outlined evolutionary sequence, some radio galaxies seem to wake up after a dormant phase of absence or much lower activity (e.g., Lara et al. 1999a). Moreover, the presence of super-massive objects in many non–active galaxies argue in favor of activity as a short transition period in most, if not all, (elliptical) galaxies, and that the "menace" for future activity is present at the center of every galaxy.

This paper is the last of a series of three devoted to the study of a sample of large angular size radio galaxies which try to address some of these open questions. Definition of the sample and radio maps in one side, and images and spectroscopic data on the other, were presented by Lara et al. (2001a, hereafter Paper I) and (2001b, Paper II), respectively. The sample, covering a sky area of 0.842 steradians[2] and spectroscopically complete at the 80%, consists of 84 radio galaxies selected from the NRAO[3] VLA[4] Sky Survey (NVSS; Condon et al. 1998) under the following selection criteria (see Paper I for details): declination above +60°, total flux density at 1.4 GHz greater than 100 mJy and angular size larger than 4′. All sources in the sample have redshift below 0.75. In this paper we present the general results of the study of the sample, with distinction between Fanaroff-Riley type I (FR I; Fanaroff & Riley 1974) and II (FR II) radio galaxies. Special attention is devoted to show the properties of GRGs, of which this sample contains 37 members.

2. General properties

2.1. FR I and FR II radio galaxies

Fanaroff & Riley (1974) distinguished two classes of radio galaxies, with clearly distinct properties: a first group (FR Is) of low power sources with radio structures dominated by the emission from the core and the jets, with lobes gradually decreasing in brightness with distance, and a second group (FR IIs) of higher power sources, with structures dominated by prominent edge-brightened radio lobes with hotspots

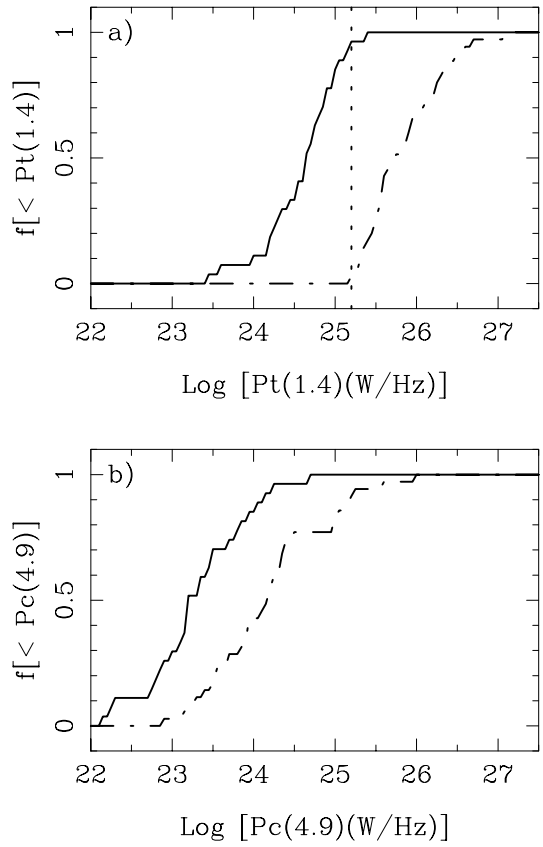

Fig. 1. a) Integrated fraction of sources with total radio power at 1.4 GHz below P_t. Continuous and dotted-dashed lines stand for FR I and FR II type radio galaxies, respectively. The vertical dotted line represents the break power between FR I and FR II radio galaxies. **b)** Integrated fraction of sources with core radio power at 4.9 GHz below P_c.

at the position where the jet impinges on the external medium. From a pure morphological distinction of the radio structure of the members of our sample, regardless of the source radio or optical luminosity, we find 31 sources (37%) which correspond to the FR I type, and 46 sources (55%) which correspond to the FR II type, of which three of them are classified as quasars. Six objects (7%) are difficult to classify in any of the two groups, showing simultaneously properties of FR I and FR II radio galaxies. We put them in an intermediate group, labeled as I/II (see Gopal-Krishna & Wiita 2001). Moreover, there is J1015+683 which results from the superposition in projection of a possibly FR I and a FR II radio sources (see Fig. 2 in Paper II).

In Fig. 1a we represent the fraction of sources with reliably measured redshift and total radio power below $P_t(1.4)$. We note how the morphologically based distinction between FR Is and FR IIs corresponds to a neat break in source total power: 96% of the FR I radio sources have $\log P_t(1.4) \leq 25.2$ (W/Hz), while 97% of the FR IIs have higher radio power. This sharp break in radio power contrasts with the result by Ledlow & Owen (1996) who find for a large sample of radio galaxies that the FR I to FR II division is a function of both, radio power and optical luminosity of the host galaxy. FR I/II radio sources, not represented in Fig. 1, fall in the region of

[2] Papers I and II erroneously mention a sky area of π steradians. However, results and discussion in those papers are not affected by this value.

[3] National Radio Astronomy Observatory.

[4] Very Large Array, operated by the NRAO.

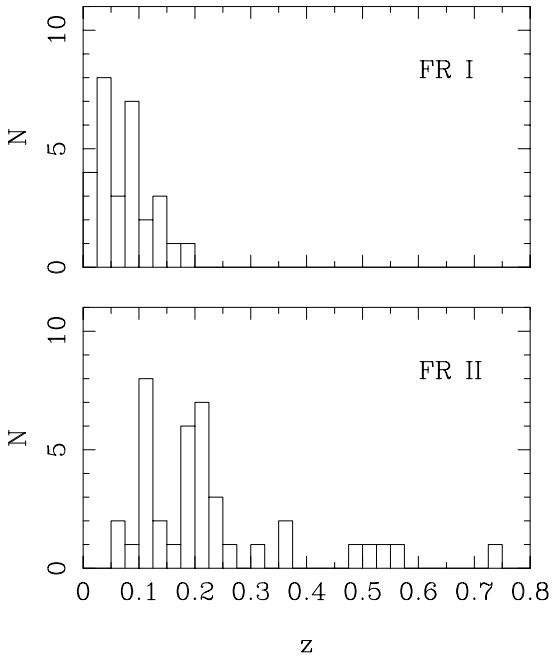

Fig. 2. Distribution of redshift in our sample for FR I (*top*) and FR II (*bottom*) radio galaxies. The redshift bin is 0.025.

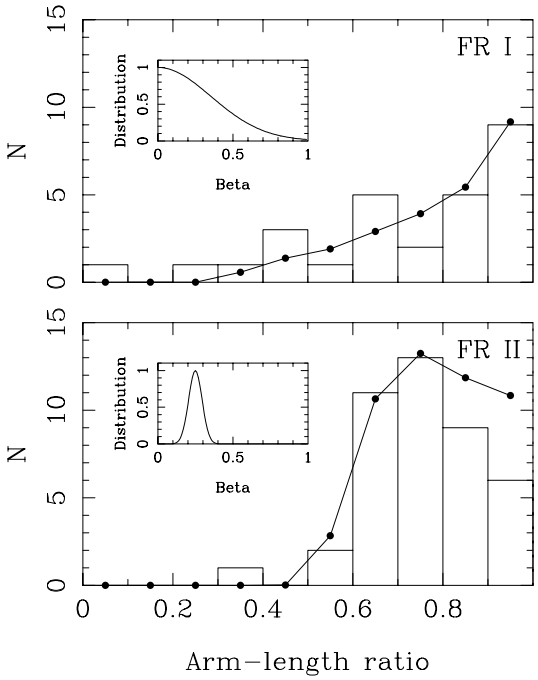

Fig. 3. Distribution of the arm-length ratio for FR I (*top*) and FR II (*bottom*) radio galaxies. The filled circles and lines represent the prediction of an orientation-based model considering the jet-head advance velocity Gaussian distribution plotted in the small frame.

transition between FR Is and FR IIs, with a mean $\log P_t(1.4) = 25.4$ (W/Hz).

Figure 1b represents the same concept as Fig. 1a, but considering the core radio power instead of the total radio power. We find that FR Is have in general weaker cores than FR IIs, but a sharp distinction in the core power of the two classes cannot be established.

Regarding the redshift distribution of the sample members, the different power and radio structure of FR I and FR II type radio sources introduce a clear selection effect. Since FR Is have low power and are diffuse and extended, surface brightness sensitivity limitations will hinder in some cases the detection of their most extended emission, preventing many FR Is to reach the $4'$ limiting size of the sample[5]. FR IIs, on the contrary, end in bright and compact hotspots, so their total size can be reliably measured. Another consequence of this fact is that FR Is with sizes larger than $4'$ are difficult to detect at large cosmological distances, since that would imply intrinsically bright extended emission, which is not usual in this type of sources. In consequence, we expect most FR Is to be at low redshift. On the other hand, for FR IIs we do not have any a priori selection effect, so in principle they can be found at low and at high redshifts. In Fig. 2 we show the distribution of redshift for the FR I and the FR II sources in our sample. As expected, we find indeed that all FR Is have $z \leq 0.2$, with a median value $\langle z_{\rm FR\,I} \rangle = 0.07$. On the other hand, the distribution with redshift of FR II radio galaxies is much broader, with a median value $\langle z_{\rm FR\,II} \rangle = 0.20$. In Sect. 5 we discuss the distribution in redshift under the perspective of the radio luminosity function.

[5] We refer to Paper I for the source size definition.

2.2. Radio source asymmetry

We define the arm-length ratio (r) of a radio source as the ratio between the length of its shorter to its longer arm. Arm-lengths were measured along the spine of the sources using our VLA maps at 1.4 GHz, or the NVSS maps when there was extended emission resolved out in our observations (see Paper I). The arm-length ratios of the members of the sample are displayed in Table 1. Errors in the determination of r are in the range of 2% to 5%, with FR I sources having larger errors than FR IIs. This is mostly due to the difficulties associated with the determination of FR I sizes through isophotal measurements (sensitivity dependent), in contrast with the metric and well defined sizes of FR II radio galaxies. But given the high sensitivity of our observations and of the NVSS, we have confidence that arm-length ratio measurements are reliable in most cases. Possible exceptions will not alter the statistics significantly.

The distribution of parameter r is plotted in Fig. 3. We find a clear difference between the distribution for FR I and FR II sources. While the distribution of the former gradually increases towards symmetry, with 50% of the sources presenting $r \geq 0.8$, the distribution of the latter appears rather concentrated around a mean value of 0.78 ± 0.14.

Apparent asymmetry is common in radio galaxies, and in principle three possible reasons could be envisaged to explain it. **First**, plasma ejection from the active nucleus could have different properties for each one of the jets (confinement, velocity, etc.) producing a different radio source morphology at each side, and in particular, a different size of each arm in the radio galaxy. **Second**, the different arm size could be due to an orientation effect. If the source is not lying on the plane of the

Table 1. Arm-length ratio (r) of the sample members.

Name	r	Name	r	Name	r	Name	r
J0109+731	0.58	J0807+740	0.91	J1504+689	0.61	J1918+742	0.37
J0153+712	0.09	J0819+756	0.70	J1523+636	0.70	J1951+706	0.79
J0317+769	0.29	J0825+693	0.89	J1530+824	0.62	J2016+608	0.60
J0318+684	0.73	J0828+632	0.57	J1536+843	0.90	J2035+680	0.66
J0342+636	0.65	J0856+663	0.71	J1557+706	–	J2042+751	0.95
J0430+773	0.88	J0926+653	0.93	J1632+825	–	J2059+627	0.90
J0455+603	0.88	J0926+610	0.66	J1650+815	0.60	J2103+649	0.70
J0502+670	0.95	J0939+740	0.91	J1732+714	0.98	J2111+630	0.55
J0508+609	0.74	J0949+732	–	J1733+707	0.92	J2114+820	0.98
J0519+702	0.96	J1015+683	–	J1743+712	0.61	J2128+603	0.65
J0525+718	0.95	J1036+677	0.78	J1745+712	0.87	J2138+831	0.47
J0531+677	0.34	J1124+749	0.58	J1751+680	0.63	J2145+819	0.98
J0546+633	0.47	J1137+613	0.80	J1754+626	0.42	J2157+664	0.09
J0559+607	0.82	J1211+743	0.67	J1800+717	0.74	J2204+783	0.79
J0607+612	0.88	J1216+674	0.73	J1835+665	1.00	J2209+727	0.92
J0624+630	0.78	J1220+636	0.75	J1835+620	1.00	J2242+622	0.83
J0633+721	0.67	J1247+673	1.00	J1844+653	0.93	J2247+633	0.89
J0654+733	0.77	J1251+756	0.79	J1845+818	0.69	J2250+729	0.84
J0750+656	0.91	J1251+787	0.47	J1847+707	0.87	J2255+645	0.92
J0757+826	0.66	J1313+696	0.77	J1850+645	0.81	J2307+640	0.82
J0803+669	0.70	J1410+633	0.78	J1853+800	0.71	J2340+621	1.00

sky, the differing light travel times to the observer for each arm will produce different sizes. And **third**, the external medium through which the jets propagate might not be isotropic, presenting different resistance to the propagation of the jets, and thus producing different size arms.

Although these three effects could act in a combined manner, we can try to constrain the possible reasons of asymmetry in our sample. First we note that the wealth of observations of the inner jets in radio galaxies and quasars do not show evidence for intrinsic differences in the properties of jets and counter-jets. The observed differences are readily explained through the effects of relativistic aberration in symmetric, antiparallel jets (e.g., Giovannini et al. 2001; Laing & Bridle 2002). In the following, we thus concentrate in distinguishing between the external medium or source orientation as the main reason of asymmetry.

We have considered a randomly oriented sample ($P(\theta) \propto \sin\theta$; P standing for probability) of intrinsically symmetric radio galaxies with a Gaussian advance velocity distribution of the jet head. Under these assumptions, we are able to obtain reasonable approximations to the shape of the observed arm-length ratio distribution solely on the basis of orientation effects for both, FR I and FR II radio sources, using different jet velocity distributions for each type of radio galaxy (see Fig. 3). But what is relevant here, our model requires too high (and thus unrealistic) jet-head advance velocities for FR Is and FR IIs. For example, a velocity distribution narrowly centered around 0.25c is required to explain the arm-length ratio distribution of FR II radio galaxies, while most models and observational data suggest much lower expansion velocities (e.g., Longair & Riley 1979; Alexander & Leahy 1987; Scheuer 1995). Moreover, even with unacceptable jet–head velocities, the model still predicts more symmetric sources than observed which might reflect the influence of the external medium not accounted for.

As a second argument, we find an strikingly large fraction (~75%) of FR II radio galaxies with a stronger lobe on the shorter arm of the radio structure. A similar behavior is also found by Machalski et al. (2001) in a sample of GRGs. To compute this percentage we have excluded quasi-symmetric sources (with $0.9 \leq r \leq 1$) to avoid confusion. We note that in an orientation based asymmetry, it is expected that the shorter arm corresponds to the receding jet and if the emission from the lobes is at least moderately beamed (e.g., Georganopoulos & Kazanas 2003), it is expected that the receding lobe presents weaker emission than the approaching one. Therefore we suggest that orientation cannot be the main reason of asymmetry.

The asymmetry could be explained if the external medium were not isotropic. In that case the shorter lobe would be the one finding stronger resistance to its expansion in the external medium, which shows up as a higher surface brightness. Supporting this idea, the sources for which we have polarization measurements present also a tendency of stronger polarized emission in the shorter and stronger lobe, consistent with a compression of the magnetic field against the external medium, but this fact needs to be confirmed through more detailed observations. Moreover, the anisotropies in the external medium most plausibly explain the existence of several sources with pairs of jets showing markedly different properties or with

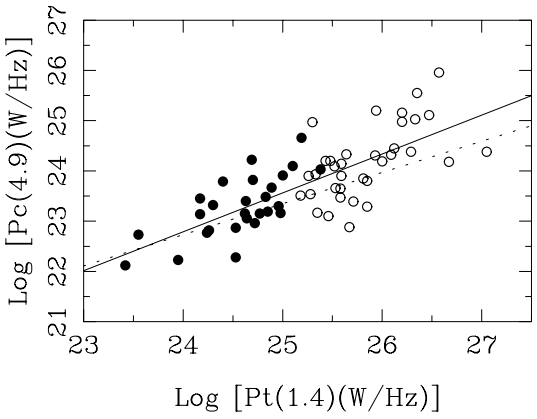

Fig. 4. Total power at 1.4 GHz vs. core power at 4.9 GHz. The continuous line represents a least squares fit to our data. The dotted line represents the correlation $\log P_c(4.9\ \mathrm{GHz}) = (0.62 \pm 0.04) \log P_t(0.408\ \mathrm{GHz}) + (7.6 \pm 1.1)$ by Giovannini et al. (2001) transformed to $P_t(1.4\,\mathrm{GHz})$, assuming an spectral index $\alpha = -0.75$. Filled and empty circles correspond to FR I and FR II type radio galaxies, respectively.

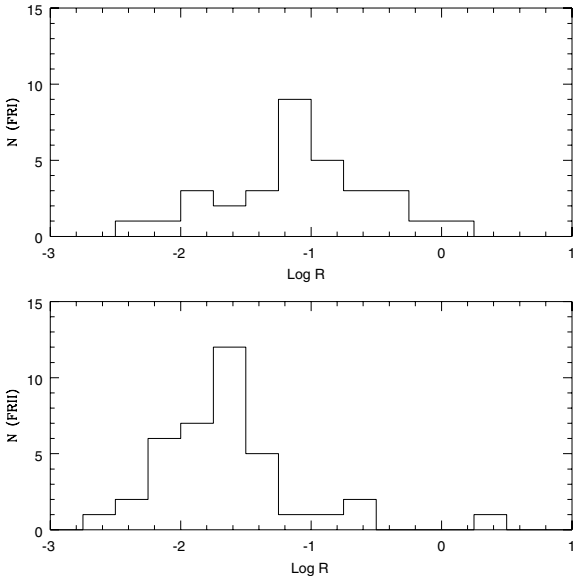

Fig. 5. Distribution of the orientation indicator R (see text) in logarithmic scales, for FR Is (*top*) and FR IIs (*bottom*) radio galaxies.

a hybrid FR I/II morphology. The most dramatic case is J2157+664 (see Paper I), with $r = 0.09$.

In conclusion, with the necessary caution required due to the uncertainties in the arm-length ratio determinations in FR Is, we obtain *i)* from the orientation based asymmetry model and *ii)* from the fact that many sources show the stronger lobe on the shorter arm, that the external medium must be the dominant effect in most of the asymmetric sources of our sample. However, we cannot exclude that orientation effects might play their role to explain certain degree of asymmetry in FR Is and FR IIs. Moreover, we do not find a clear dependence of the arm-length ratio of FR IIs with the source size.

2.3. Radio core properties

A compact radio core is detected at 4.9 GHz in 100% of the sources in the sample. The core spectral index[6] distribution of the whole sample has $\langle\alpha\rangle = -0.10 \pm 0.47$. If we consider separately the FR I and the FR II type radio galaxies, we find $\langle\alpha_{\mathrm{FR\,I}}\rangle = -0.24 \pm 0.52$, while $\langle\alpha_{\mathrm{FR\,II}}\rangle = 0.07 \pm 0.41$. We ascribe the different mean values of the two families of radio galaxies to the fact that the radio core in FR Is cannot be isolated from the jets as neatly as in FR IIs. In consequence, the core spectral index in FR Is suffers from more contamination from the steeper jet emission than FR IIs. This result is consistent with that found in the B2 sample (de Ruiter et al. 1990).

In Fig. 4 we display the core radio power at 4.9 GHz as a function of the total radio power at 1.4 GHz. We find a correlation between these two parameters of the form

$$\log P_c(4.9) = (0.77 \pm 0.08) \log P_t(1.4) + (4.2 \pm 2.1).$$

This correlation is steeper than that of Giovannini et al. (2001; dotted line in Fig. 4, where we have transformed Giovannini's correlation from $P_t(408\ \mathrm{MHz})$ to $P_t(1.4\ \mathrm{GHz})$ assuming a spectral index $\alpha = -0.75$), but it is still consistent with it. As discussed by several authors (e.g., Giovannini et al. 1994) the prominence of the core with respect to the total radio emission can be considered as an indicator of orientation of the nuclear jet, and, more generally, of the whole radio source with respect to the observer.

Morganti et al. (1993) define as an orientation parameter the ratio $R = S_{\mathrm{core}}/(S_{\mathrm{tot}} - S_{\mathrm{core}})$, i.e. the ratio between the flux density of the core and the flux density of the extended structure, both at 1.4 GHz. We have derived this parameter for our sample, and show in Fig. 5 the histogram of $\log R$ for the FR I and the FR II classes. We find that the FR Is are characterized by more dominant cores, and the median values are $\log R = -1.09$ for the FR Is and $\log R = -1.64$ for the FR-IIs. The probability that the two histograms are drawn from the same population is less than 0.1%, checked with the Kolmogorov-Smirnov test. The different behavior of the two classes is in the same direction as the weak difference detected by Morganti et al. (1993). It could reflect the fact that the core flux density in FR Is is more likely to be affected by the jet emission than in FR IIs (the same reason argued to explain the spectral index difference), and also that the core radio power in radio galaxies does not increase linearly with the total radio power in agreement with the slope of the existing correlation between the core luminosity P_c and the total luminosity P_t.

A more reliable parameter to define the core prominence is then obtained using the core emission at 4.9 GHz. Moreover, given the P_c vs. P_t correlation, expected if sources are in energy equipartition conditions (see Giovannini et al. 2001), it is useful to use as orientation indicator a parameter, P_{CN}, defined as the ratio between the observed core luminosity (P_c) and the core luminosity expected from the P_c vs. P_t correlation (P_{cm}). The median value of the core luminosity P_{cm} at 4.9 GHz as a function of the total power P_t at 1.4 GHz is given for a large sample of radio galaxies and quasars by the relation $\log P_{\mathrm{cm}} = 0.62 \log P_t + 8.0$ obtained by Giovannini et al. (2001) and scaled here to the total power at 1.4 GHz using a

[6] The spectral index α is defined so that the flux density $S \propto \nu^{\alpha}$.

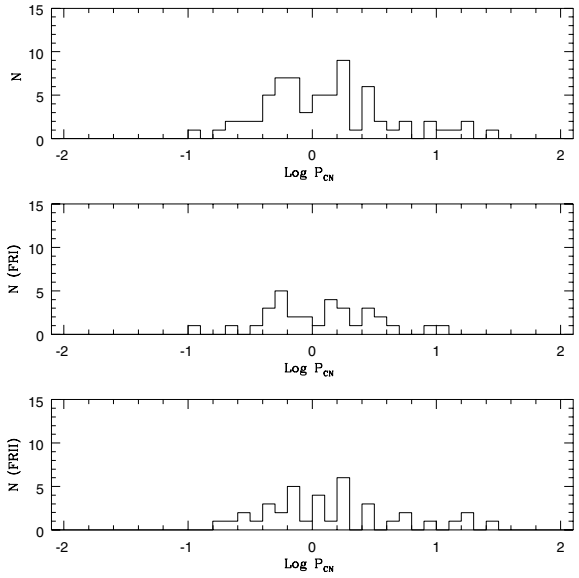

Fig. 6. Distribution of the orientation indicator P_{CN} (see text) in logarithmic scales, for the whole sample (*top*), FR Is (*middle*) and FR IIs (*bottom*) radio galaxies.

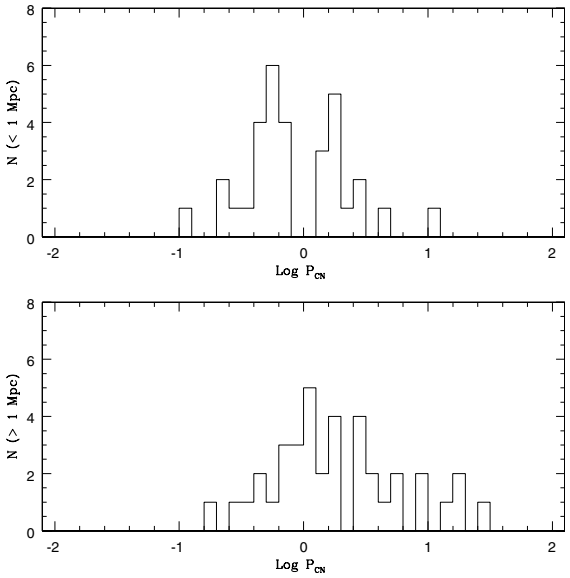

Fig. 7. Distribution of parameter P_{CN} in logarithmic scales for sources with projected linear sizes smaller (*top*) and larger (*bottom*) than 1 Mpc.

spectral index $\alpha = -0.75$. We then calculate $P_{CN} = P_c/P_{cm}$. Considering that in a randomly oriented sample as that of Giovannini, the average orientation angle with respect to the observer corresponds to 60°, in presence of relativistic beaming effects we expect that sources with the angle between jet axis and line of sight <60° or >60° show $P_{CN} > 1$ or <1, respectively.

The distribution of P_{CN} for the whole sample is given in the top panel of Fig. 6, whereas the middle and bottom panels show the distributions for the FR I and FR II classes, respectively. We note that, although Figs. 6 and 7 display the distribution of $\log P_{CN}$, the considerations in the following text refer to the values of P_{CN} (not to their logarithm). We find a large number of sources with $P_{CN} > 1$, i.e. with a core power larger than expected from their total power (the median of P_{CN} for the whole sample is 1.22). The same behavior is found for the FR I and FR II classes, with no statistically significant difference between the two distributions, on a Kolmogorov-Smirnov test (medians of the FR I and FR II sources are 1.25 and 1.21, respectively). This indicates that the sample under study contains an excess of sources which, according to the standard interpretation, would be oriented at angles smaller than 60°.

This result is quite unexpected, since sources with large apparent linear sizes are expected to be poorly affected by projection effects, i.e. preferentially oriented at large angles to the line of sight. In addition, we would also expect that the sources with the larger projected linear size are those with a P_{CN} smaller than 1. This is contrary to the observations. In fact, by analyzing the distribution of P_{CN} in the sources with projected linear size smaller and larger than 1 Mpc, we find that the latter have an excess of values of $P_{CN} > 1$ (see Fig. 7). The same trend is deduced by the plot of the parameter P_{CN} versus the source linear size (see Fig. 8, where FR I and FR II are indicated as full and empty circles, respectively). The statistical difference between the two distributions is at the confidence level

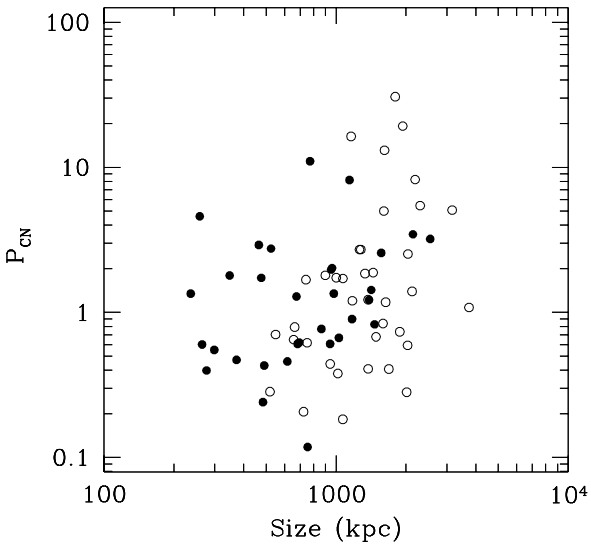

Fig. 8. Orientation indicator P_{CN} as a function of linear size. Symbols represent the same as in Fig. 4.

of about 2% on a Kolmogorov-Smirnov test. We note that the major source of uncertainty in the estimation of P_{CN} is related to the radio galaxy core variability. Assuming a core variability of a factor 2 (much larger than the core variability observed in most radio sources) we have an uncertainty of 0.3 in $\log P_c$. However this is the uncertainty related to a single object; assuming a random core variability we estimate the possible uncertainty for Figs. 6 and 7 to be about 0.1.

The difference in the distribution of P_{CN} between sources of size smaller and larger of 1 Mpc is at a marginal level of statistical significance. However, it is interesting to note that it is in line with the predictions of the the evolutionary effects detected by Ishwara-Chandra & Saikia (1999) and by Schoenmakers et al. (2001), and discussed in Sect. 2.6. According to these authors, the total luminosity of a radio source decreases as it

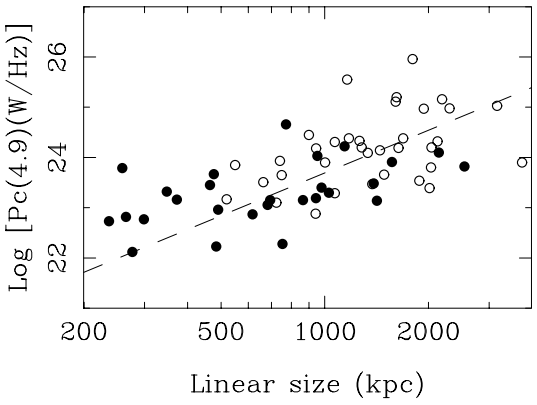

Fig. 9. Apparent correlation between the core radio power and the source linear size, induced by the sample biases. The dashed line represents the influence of the selection criteria and of the $P_c(4.9)$ vs. $P_t(1.4)$ correlation in this plot. Symbols represent the same as in Fig. 4.

expands to very large dimensions. As a consequence, its nucleus would appear more prominent than expected from pure orientation effects. From our data, there is indication that the P_c vs. P_t correlation is in support of a luminosity evolution in giant radio sources. We can roughly estimate that an increase of 10 to 100 times in the total power of GRGs would lead to values of $P_{CN} \sim 1$ for these sources. Note that a two order of magnitude increase in the total power of GRGs would also be consistent with the power-size diagram in Fig. 11.

We finally note that apparent correlations of the core radio power with the source redshift and linear size are entirely due to biases introduced in the sample selection through the flux density and the angular size limits, and to the correlation between the total and the core radio power (Paper I). This bias arises from the need for larger sources to have more flux density to exceed the minimum surface brightness limit of the NVSS. As an example, we show in Fig. 9 the core power as a function of the source linear size, which could be interpreted as sources being intrinsically larger due to an unusually higher core power (Gopal-Krishna et al. 1989). However, the dashed line represents how the limits in flux density and angular size translate into this plot, taking also into account the total power vs core power correlation mentioned above. We note that it is fully consistent with the observed trend, so that it is possible to conclude that the source size is unrelated to the core power, in agreement with studies on GRGs (Ishwara-Chandra & Saikia 1999). It could also be argued that the core power vs. source size is a physically meaningful correlation, and that from the biases introduced through the selection criteria we could derive the total vs. core power correlation. To isolate the problem in our sample is not easy since we have both, flux density and angular size limits in our sample definition, but we note that biases induced correlations depend strongly on the adopted selection criteria. However, consistent correlations of the total vs. core power have been obtained with well defined complete samples including compact and giant radio sources as well as quasars and radio galaxies (see e.g. Giovannini et al. 1988, 2001; de Ruiter et al. 1990).

2.4. The orientation of the sample members

One of the aims of this work was to select a sample of radio galaxies with their jets oriented near the plane of the sky for a subsequent study of the parsec scale properties of these jets. Although reliable limits to the orientation of the members of our sample with respect to the observer cannot be derived from current data, two lines of argumentation favor the idea that these sources have moderately large angles of orientation. First, statistics of radio quasars: we find in our sample 3 objects out of 46 with FR II radio structure which are classified as quasars (Paper II). If we consider that the probability of finding an object with a certain angle θ to the line of sight is $P(\theta) \sim \sin\theta$, we can estimate the expected number of quasars in a randomly oriented sample if quasars are assumed to have orientation angles below 38° (Urry & Padovani 1995). This number is ∼10 for a sample of 46 FR II radio galaxies, more than three times larger than found in our sample, which means that most objects must have orientation angles well above 38°. And second, source intrinsic linear sizes: with a mean projected linear size of 1.02 Mpc in our sample, orientation angles below 20° can, with a high degree of confidence, be discarded for most objects in order not to have intrinsically too large radio galaxies, which are not observed in other samples.

However, we have found (Sect. 2.3) that the correlation between the core power and the total radio power is consistent with that derived by Giovannini et al. (2001) for a sample of randomly oriented radio galaxies. The distribution of the orientation indicator P_{CN} is consistent with a large number of sources with orientation angles below 60°, which is against our preconceived idea about the orientation of the sample members. However, as we have seen, this result could simply be a consequence of the evolution of radio galaxies which undergo a diminution of the power of their radio lobes power as they expand.

2.5. The host galaxies

As expected, the host galaxies of the sample members for which a brightness profile could be derived (35% of the sample) are consistent with being of elliptical morphology (see Paper II). In Fig. 10 we show histograms of the effective radius derived by fitting a $r^{1/4}$ profile to the brightness distribution, separated for FR I and FR II type radio galaxies. Although the statistics are rather poor, FR I radio galaxies tend to have larger effective radius than FR IIs, consistent with the result by Govoni et al. (2000) obtained from a detailed study of a sample of low redshift radio galaxies. These authors also find that the hosts of FR I radio galaxies are more luminous than the hosts of FR IIs (see also Owen & Laing 1989).

Laing & Bridle (2002) present strong evidence that the deceleration of the jets in the low luminosity radio galaxy 3C 31 is produced by a mechanism of entrainment of thermal matter in a dense interstellar medium (ISM) across the jets boundary. If the ISM density is directly related to the observed luminosity (i.e., more material coming from stellar mass losses), then the luminosity difference in FR Is and FR IIs could be an indirect measure of the degree of deceleration in the jets of these

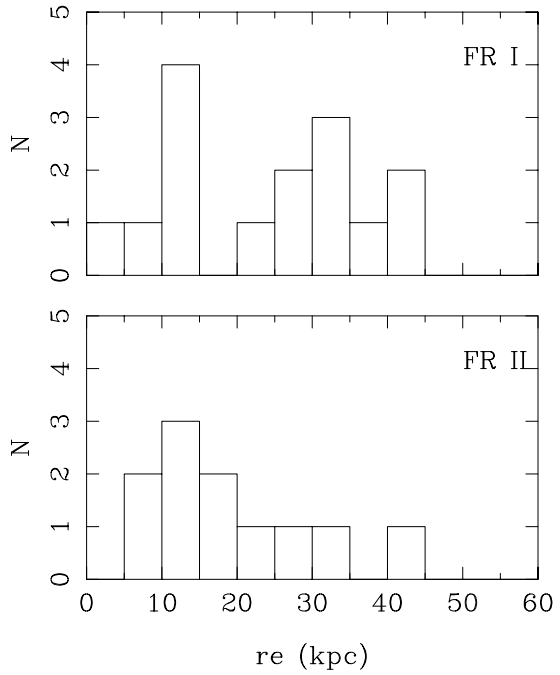

Fig. 10. Distribution of the effective radius of the host galaxies observed at optical wavelengths (Paper II).

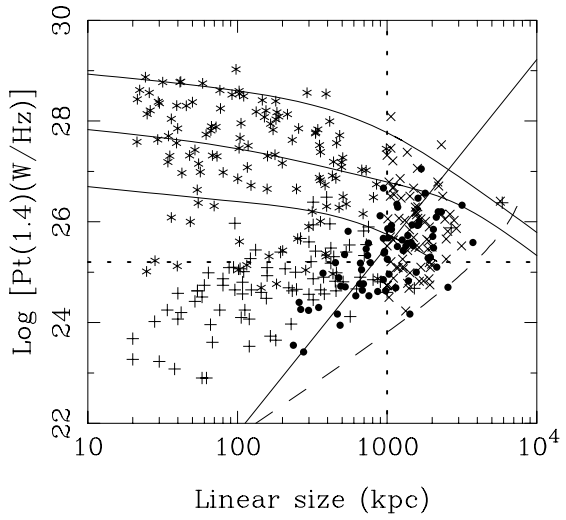

Fig. 11. Power–size diagram of radio galaxies. Filled circles correspond to our sample; crosses correspond to the B2 sample; x-shaped crosses correspond to a compilation of GRGs (Ishwara-Chandra & Saikia 1999; Schoenmakers et al. 2000a; Machalski et al. 2001); asterisks correspond to the Peacock & Wall (1981) sample. The dashed line represents the sensitivity limit of the NVSS for a 16′ extended 100 mJy source (see Paper I). The horizontal dotted line marks the power break between FR I and FR II radio sources. The vertical dotted line marks the definition of GRGs. The curved continuous lines represent evolutionary tracks for sources with jet powers of (*top to bottom*) 1.3×10^{40}, 1.3×10^{39} and 1.3×10^{38} W from Kaiser et al. (1997). The straight continuous line represents the trend imposed by our selection criteria in flux density and source angular size.

objects. Moreover, the higher luminosity of FR Is with respect to FR IIs might be related to the separation between the two types of radio galaxies being also dependent on optical luminosity (Ledlow & Owen 1996). However, Govoni et al. (2000) find a very large scatter in the radio – optical luminosity plane and, unfortunately, we have no reliable data on optical luminosity for our sample to make a similar study. But this idea contrasts with the sharp FR I/II break we find in radio power, independently of optical luminosity (Sect. 2.1).

If we consider all the galaxies in our sample with spectroscopic information, we find that 65% of the FR I type radio galaxies have optical spectra characterized by absorption lines only. On the other hand, 71% of FR II type radio galaxies show emission lines in their optical spectra. This result is consistent with the unified model of radio sources (e.g., Antonucci et al. 1993), which relates FR I radio galaxies with BL-Lacs (generally without strong emission lines) and FR II radio galaxies with radio quasars (with prominent emission lines). But it also brings up the question about the FR I-FR II dichotomy, since this result connects the type of large scale radio structure with the properties of the optical spectrum in the active core of the galaxy.

The differences in the spectral properties between the two families of radio galaxies do not correspond with different properties in the parsec scale jets observed with VLBI, which present similar radio structures and evidence of relativistic flows (e.g., Giovannini et al. 2001). However, radio observations at sub-kiloparsec scales show that the differences between the two families of radio galaxies might arise at distances of a few hundreds of parsecs from the central core (e.g., Lara et al. 1999b), a size coincident with that estimated for the narrow line region in Seyfert galaxies (Netzer 1990).

Baum et al. (1995) conclude, from the study of a sample of FR I and FR II type radio galaxies, that while emission-line gas in FR IIs is photoionized by nuclear UV continuum from the AGN, in FR Is the emission line gas is most possibly energized by the host galaxy itself. They argue as most plausible that there is a fundamental difference in the central engines (accretion rate) and/or immediate accretion region around the engine in FR I and FR II radio galaxies. In a similar fashion, Ghisellini & Celotti (2001) suggest that the FR I-FR II dichotomy is mainly controlled by the properties of the accretion process, and even consider the possibility of an FR II to FR I evolution of individual objects in some cases (see Sect. 5). Chiaberge et al. (2000) observe a sample of FR I radio galaxies with the HST and affirm that "the innermost structure of FR I radio galaxies differs in many crucial aspects from that of the other classes of AGN; they lack the substantial BLR, tori and thermal disc emission, which are usually associated with active nuclei", and suggest that in FR Is "accretion might take place in a low efficiency radiative regime".

Arguments which try to explain the FR I-FR II dichotomy based solely on differences of the central engine are not free from difficulties: first, the similar properties between parsec scale jets in FR I and FR II radio galaxies imply the same (or very similar) jet production mechanism for both types of sources, and second, the existence of FR I/II sources with large scale properties common with FR I and FR II radio galaxies (Gopal-Krishna & Wiita 2001). We support the idea that

the central kiloparsec region surrounding the active core must also play, together with the central engine, a crucial role in the FR I-FR II dichotomy. It is in this region where differences in the radio structures of the two families of radio galaxies become evident and where the emission lines in the optical spectra are produced. Moreover, the properties of this region must be closely linked with the conditions in the region of accretion, which define the source of ionization or the different core power. In a small fraction of sources, the external medium at larger scales (possibly at the galactic halo) might determine key properties of the large scale radio structure (FR I/II sources, or environment induced asymmetry).

2.6. The power–size diagram

The relation between the intrinsic size and the radio power of radio galaxies is a powerful tool for studying the evolution of radio galaxies (Shklovskii 1963; Scheuer 1974; Neeser et al. 1995; Kaiser et al. 1997). We display in Fig. 11 the power−size diagram for a large compilation of radio galaxies taken from the B2 sample, the Peacock & Wall (1981) sample, our sample of large angular size radio galaxies (Paper I), and a compilation of GRGs from Ishwara-Chandra & Saikia (1999), Schoenmakers et al. (2000a) and Machalski et al. (2001). Both FR I and FR II radio galaxies are represented in this plot. In order to separate the influence of the sample selection criteria and of the evolution of radio galaxies we have plotted also a line representing the sensitivity limits affecting our sample, as discussed in Paper I. This sensitivity limit mostly affects the selection of FR I radio galaxies, and in principle of very large FR IIs. We also plot the evolutionary tracks of FR II radio galaxies determined by Kaiser et al. (1997) from a model of the cocoon of FR II radio galaxies which takes into account the energy loss processes for the relativistic electrons. The lines plotted correspond to their Fig. 1, for three different jet powers, and to the case when the energy of the magnetic field and of the particles is in equipartition (their case 3). This model explains the dearth of high luminosity GRGs, even if recent systematic searches of GRGs are reaching lower and lower sensitivity limits (Paper I; Schoenmakers et al. 2000a; Machalski et al. 2001). Moreover, the energy losses in the radio lobes of extended radio galaxies might also explain the relatively high core prominence in these objects (Sect. 2.3).

Note that the apparent correlation between the radio power and the source size in our sample (filled circles in Fig. 11) is well reproduced taking into account the biases introduced by the sample selection criteria in total flux density and angular size, thus the need of considering several samples with different selection criteria to derive valuable conclusions from power-size relations.

The lack of high power GRGs is well visible in Fig. 11 and confirmed by the large sample of radio sources: in the linear size range <1 Mpc we have many sources with radio power between 10^{29} and 10^{28} W/Hz, while very few GRGs have radio power $>10^{27}$ W/Hz. It cannot be justified by selection effects. A lack of giant radio sources is expected by evolutionary models of radio sources (Kaiser et al. 1997; Blundell et al. 1999).

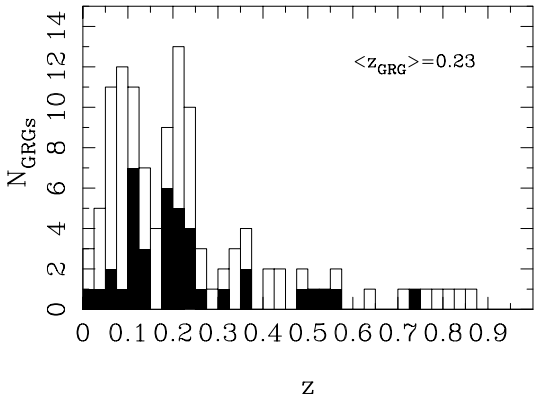

Fig. 12. Distribution of redshift of giant radio galaxies. The white histogram corresponds to a compilation of 115 GRGs (see text for references). The black histogram corresponds to the GRGs in our sample.

We estimate that a radio power loss of a factor 10 to 100 is required from the size–power relation. This loss is in remarkably agreement the total radio power loss expected from the P_c vs. P_t correlation (see Sect. 2.3).

3. The giant radio galaxies

We summarize here the results presented in previous sections, but from the point of view of giant radio galaxies. To improve the statistics of this type of radio galaxies, we consider when possible a compilation of 115 GRGs taken from Ishwara-Chandra & Saikia (1999), Schoenmakers et al. (2000a), Machalski et al. (2001), and our sample (Paper I) (the same compilation shown in Fig. 11).

From Fig. 11 we find that most GRGs have sizes below 3 Mpc, with only a limited number of objects surpassing this size. A cutoff in the linear size of GRGs was already noted by Ishwara-Chandra & Saikia (1999) from the analysis of a sample of 50 GRGs, and by Schoenmakers et al. (2001) from a sample of 47 GRGs. Our sample helps to confirm this cutoff between 2 and 3 Mpc, although we note it might be a combined effect of the decrease in luminosity with source size (Kaiser et al. 1997), the sensitivity limitation of the NVSS and the bias introduced by our selection criteria (see Fig. 11).

In Fig. 12 we plot the distribution with redshift of the GRGs in our sample, together with the same distribution for the compilation of GRGs. We find that most known GRGs have a redshift $z \leq 0.25$. In our sample we know it is mostly due to our selection criteria: we do not select sources smaller than 1 Mpc at $z > 0.2$, and the minimum selectable size increases rapidly with z (see Paper I). That means that at $z > 0.2$ many GRGs are being missed and only those with sizes of about 2 Mpc or larger can be selected, but these are rare objects. Moreover, most (∼77%) of the GRGs in our sample are FR II type radio galaxies. This is not unexpected because of the properties of FR I radio galaxies: first, they have lower power than FR IIs, and second, their surface brightness decreases rapidly with distance from the activity center, so sensitivity limitations make difficult to observe their emission at very large distances from the core.

If we compare the arm-length ratio, r, of the GRGs of FR II type in our sample with that of the FR IIs in the whole sample, we do not find any significant difference. GRGs have an average $r = 0.79 \pm 0.14$, fully consistent with the value obtained for the whole sample ($r = 0.78 \pm 0.14$). In consequence, we do not find evidence that GRGs are more asymmetric than smaller galaxies, in contrast with Schoenmakers et al. (2000a).

There are several circumstances one can think of which might help a radio galaxy to become a GRG: *i)* a lower density external medium so that the expansion of the radio source is not hampered; *ii)* an older age to allow the radio galaxy to expand over large distances; or *iii)* a higher core power to provide the jets the necessary thrust to reach Mpc scales. Our sample allows us to compare the core power of GRGs and smaller radio galaxies. Figure 9 shows the apparent correlation between core radio power and source size. Since this correlation can be fully explained by the biases introduced in the sample selection through the flux density and the angular size limits (Sect. 2.3), it is not possible to conclude that GRGs have more powerful cores than smaller radio galaxies. On the other hand, spectral aging analysis suggest that GRGs are the older population of normal FR I and FR II radio galaxies (Mack et al. 1998; Schoenmakers et al. 2000a). But time alone is not sufficient if the external medium is very dense. We suggest that it must be the combination of two ingredients, an old age and a low density environment, which results in a giant radio galaxy.

4. Cycles of activity in radio galaxies

If the activity of a radio-loud AGN is the result of accretion of matter onto a compact massive object, likely a black hole, then it is reasonable to assume that the life of a radio source is determined by the accretion rate. It should be then expected to find in samples of radio galaxies a significant number of sources with signs of having passed through periods of different degrees of activity produced by possible changes in the accretion rate.

We detect a compact radio core in 100% of the radio galaxies in our sample, a fact that can be interpreted as core activity currently present in all selected objects; there are no switched-off cores, with perhaps the exception of J2111+630, a large angular size FR II type radio galaxy with a very weak core and no evident hotspots in its radio structure (see Paper I, but unfortunately its redshift could not be determined so the radio power could not be evaluated).

In our sample we do find objects, with active cores, but that present signs of different phases, or cycles, of activity: J0317+769 (FR I), J1745+712 (FR II), J1835+620 (FR II), J2035+680 (FR I) and J2340+621 (FR I) (see Paper I for images of the radio sources):

- J0317+769 presents a small FR I type morphology, with well defined lobes, and a long and diffuse tail which could be the result of an older period of activity.
- J1745+712 shows a FR II type structure without evident hotspots, and a small bright and symmetric ejection which might be the consequence of an enhancement of the activity.
- J1835+620 has two symmetric bright components within a typical FR II structure (Lara et al. 1999a).
- J2035+680 is a FR I radio source with a very bright knot of emission in one of the jets, and diffuse extended, probably older, emission beyond.
- J2340+621 presents a typical FR I radio structure, with symmetric and bright knots of emission which might be the consequence of an enhancement of the core activity.

We note that reactivation, as we consider it here, is a more general phenomenon than the "double-double" morphology described by Schoenmakers et al. (2000b), which can be considered as a particular case within which only the radio source in our sample J1835+620 properly fits.

The physical conditions under which a radio source can experiment a process of reactivation are not known. It is believed that interaction and merging with neighboring galaxies can be critical for this, providing an efficient mechanism to remove angular momentum and directing gas towards the active center of the galaxy (Bahcall et al. 1997). However, we only find nearby companions in two of the previously mentioned galaxies (J0317+769 and J1835+620, see Paper II). A much more detailed optical study of the host galaxies with high angular resolution is necessary to reach definite conclusions about the relation between merging and reactivation of the radio emission.

5. FR II to FR I evolution?

In this section we address the question raised by several authors (e.g., Baum et al. 1995; Ghisellini & Celotti 2001) about the possibility of an FR II type radio galaxy evolving into an FR I type source. For that, we compare the predictions derived from the radio luminosity function (RLF) with our observations. Given that our sample consists of large size objects, and for that reason probably older than objects in other samples (from which the RLF is determined), we expect that if such evolution exists it will manifest itself in an evolved sample like ours, in the sense of having an over-population of FR Is and fewer FR IIs than expected from the RLF.

We have used the Dunlop & Peacock (1990) RLF at 2.7 GHz. To choose one among the several models presented by these authors is irrelevant at the redshifts involved in our sample, since all models are well constrained by the local RLF. We have used their free-form model 5, which provides the best results for the LBDS Hercules sample of mJy radio sources (Waddington et al. 2001). In the RLF, we have introduced the area of our survey and the flux density limit of the sample transformed to 2.7 GHz assuming a spectral index $\alpha = -0.75$. We have also compared the results with the recent RLF determined by Willott et al. (2001) at 151 MHz. As expected for radio sources with redshift below 1, both RLFs provide similar results.

We define the parameter x as the difference in the number of FR II and FR I radio sources divided by the total number of radio sources per redshift interval of 0.05. This parameter illustrates the relative abundance of FR Is and FR IIs in the sample, and how this relative abundance varies with the redshift. If all sources are of FR II type, then $x = 1$; if there are only FR I type

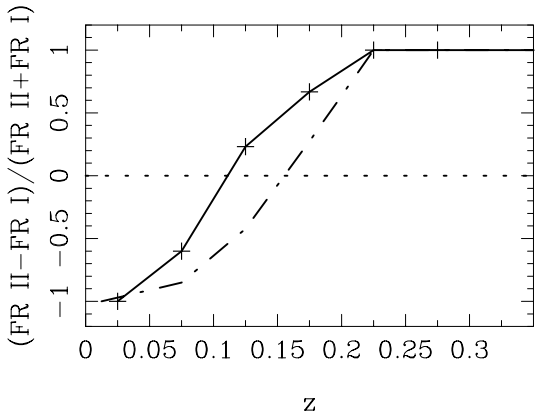

Fig. 13. Relative number of FR I and FR II type radio galaxies as a function of redshift. The continuous line represents the result obtained from our sample. The dashed line is the result obtained from the Dunlop & Peacock (1990) RLF.

radio galaxies, then $x = -1$. In Fig. 13 we display the parameter x in the redshift range 0 to 0.35. At higher redshifts $x = 1$, since we do not detect FR Is. From the RLF we have computed, for each redshift interval, the number of sources with radio power below and above the break power that separates neatly the two families of radio galaxies (Sect. 2.1), and obtained the value of x and its dependence with redshift. It is not possible to introduce in the RLF the angular size limit of our sample, so we assume that x does not depend on the source angular size (see note of caution below).

We obtain that the RLF predicts well the lack of FR IIs at low redshift, and the absence of FR I type radio galaxies at redshifts above 0.25. However, from our data we find a larger number of FR II type radio galaxies than predicted by the RLF. This result is not consistent with an evolution of individual radio galaxies from FR II to FR I type since in that case we should obtain the opposite result in an evolved sample like ours: a larger abundance of FR Is. This result, that is, the lack of evidence of a FR II to FR I evolution, might be influenced by at least two factors: first, it is not possible to discard a dependence of the parameter x with the radio source size, which might be partially masking the conclusions; second, but related, the overabundance of FR II radio galaxies might be the result of a bias in the selection of FR I radio galaxies due to sensitivity limitation in the detection of extended emission.

In Fig. 14 we display the number of radio galaxies per redshift bin of 0.05, and compare the observational results with the predictions of the RLF. As mentioned previously, the RLF cannot deal with an angular size limit of 4′ but we try here to estimate which is the fraction of radio galaxies with angular sizes above this value, comparing the RLF with our observations. In Fig. 14b, we show the number of FR I radio galaxies per redshift bin. We find that the RLF, restricted to FR Is and scaled by a factor of 0.047 predicts well the observed number of FR I objects at a redshift $z \sim 0.1$, where we do not expect to have missed a significant number of large sources in our sample due to the lack of sensitivity to very extended emission (Paper I, Fig. 6). Similarly, in Fig. 14c, we present our observed results for FR II

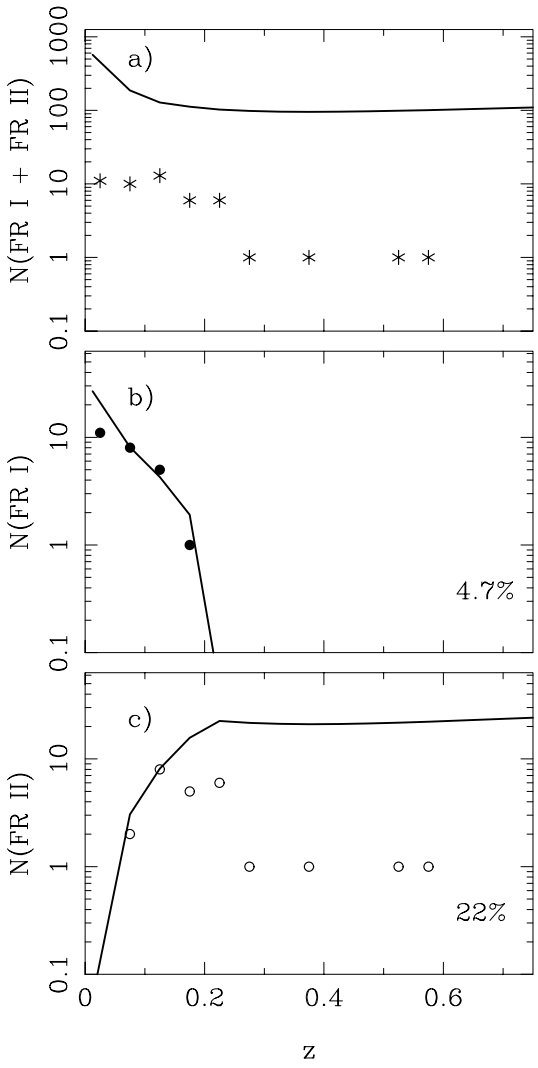

Fig. 14. a) Number of radio sources with flux density at 1.4 GHz above 100 mJy and angular size above 4′ per redshift bin of 0.05 obtained from our sample (asterisks). The continuous line represents the number of sources with flux density above 100 mJy at 1.4 GHz and unconstrained angular size obtained from the Dunlop & Peacock RLF. **b)** Filled dots represent the same as asterisks in **a)**, but only considering FR I type radio galaxies. The continuous line represents the number of FR I type radio galaxies from the RLF, scaled by a factor of 0.047. **c)** Same as **b)**, but for FR II type radio galaxies. The continuous line results from the RLF after applying a scaling factor of 0.22.

radio galaxies, and how the RLF, restricted to FR II radio galaxies and scaled by a factor of 0.22 fits the observations at the same redshift range. If we take into account the degree of spectroscopic completeness of our sample (80%; Paper II) and assume that this completeness distributes uniformly at all redshift bins (which is probably not correct), the above factors change to 0.059 (∼6%) and 0.28 (∼28%) for FR Is and FR IIs, respectively. At redshifts higher than $z = 0.1$, the RLF over-predicts the number of FR IIs, which is not unexpected considering that, for example, at $z = 0.4$ an angular size greater than 4′ implies a linear size larger than 1.5 Mpc, and such large sources are very rare (Sect. 3).

We can conclude that about 28% and 6% of the FR II and FR I sources, respectively, at a redshift of about 0.1 and with a flux density above 100 mJy ($\log P_t(1.4) \geq 24.65$) have angular sizes larger than 4′. Considering Fig. 1a, we find that all FR IIs and about half of the FR Is are above this power level. Therefore, 28% of all FR IIs and about 3% of all FR Is at $z \sim 0.1$ have angular sizes larger than 4′. Considering only FR II type radio galaxies whose physical size can be well determined from radio observations, that means that about one out of four FR II sources have linear sizes larger than 500 kpc, that is are in an advanced stage of evolution. For example, assuming an expansion velocity of 0.1c, one out of four FR II radio galaxies would be older than ∼10 Myrs. For typical GRG ages of a few tens of Myrs, we infer from our analysis that a large fraction of FR II radio galaxies (about 70%) are younger than this and that radio loud activity is a short-lived process in AGNs.

6. Conclusions

We present in this paper, the last of a series of three, the general properties of a sample of 84 radio galaxies selected from the NVSS, with total flux density at 1.4 GHz ≥ 100 mJy, declination above +60° and angular size larger than 4′. This study is based on radio (Paper I) and optical (Paper II) observations of the sample members. The main conclusions of our work can be summarized as follows:

- From a pure morphological distinction of the sample members according to its FR I or FR II type morphology, we confirm that both groups are separated by a break in the total radio luminosity, at $\log P_t(1.4\ \mathrm{GHz}) = 25.2$ (W/Hz).
- There is a small population of radio sources (7% in our sample) which show simultaneously properties of FR I and FR II radio galaxies, with a mean total radio power in the region of transition between the FR I and FR II families.
- We find that asymmetry in the structure of FR I and FR II radio galaxies can be explained as due to anisotropies in the medium through which the jet propagates. Arguments based on orientation effects would require too high jet-head advance velocities.
- FR I radio galaxies have in general lower power cores than FR II radio galaxies, although the distinction is not as clear as in the total radio power. There is a correlation, independent of the FR I-FR II dichotomy, between the core and the total radio power, consistent with that derived by Giovannini et al. (1988, 2001). The prominence of the radio cores in our sample (evidenced through the P_{CN} orientation indicator) can be explained as a result of the evolution of extended radio galaxies. The evolution of extended radio galaxies implies a total power decrease in GRGs of a factor 10−100, in agreement with Kaiser et al. (1997).
- Considering the known properties of FR I and FR II radio galaxies at parsec, subkiloparsec and megaparsec scales, and the properties of their optical spectra, we suggest that the central kiloparsec region plays a crucial role in explaining the FR I-FR II dichotomy, where differences in the radio structure between the two families seem to appear and whose properties might determine the presence or not of emission lines. We note however that the properties of this region are surely linked with the properties of the accretion disk which ultimately determines the source of ionization and the different core radio power in FR I and FR II sources, but apparently not the jet production mechanism.
- The luminosity tracks predicted by the model of Kaiser et al. (1997) explains well the dearth of high luminosity and large size radio galaxies. Our study and other recent searches of GRGs, even if much more sensitive and systematic than previous works on large size radio galaxies, do not find high luminosity giant sources.
- We do not find evidence of the GRG phenomenon as being due to stronger core radio power. Our observations are consistent with GRGs as the older population of normal FR I and FR II radio galaxies expanding in low density environments.
- A compact radio core is detected in 100% of the sample members, indicating that core activity is present in all objects. However, we find in our sample 5 objects with signs at kpc scales of having passed through different phases of activity. Nearby galaxies are found in two of these "reactivated" objects, but more detailed observations are required to study the role of galaxy merging in triggering different cycles of activity.
- Comparing the FR I and FR II abundances as a function of redshift with the predictions of the RLF, we do not find evidence of a possible FR II to FR I evolution of radio galaxies.
- From the RLF and our sample, we find that about one out of four FR II type radio galaxies with $z \sim 0.1$ have linear sizes larger than 500 kpc, thus being in an advanced stage of evolution.

Acknowledgements. This research is supported in part by the Spanish DGICYT (grants AYA2001-2147-C02-01). L.F. and G.G. acknowledges the Italian Ministry for University and Research (MURST) for financial support under grant Cofin 2001-02-8773. The National Radio Astronomy Observatory is a facility of the National Science Foundation operated under cooperative agreement by Associated Universities, Inc.

References

Alexander, P., & Leahy, J. P. 1987, MNRAS, 225, 1
Antonucci, R. 1993, ARA&A, 31, 473
Bahcall, J. N., Kirhakos, S., Saxe, D. H., & Schneider, D. P. 1997, ApJ, 450, 486
Baum, S. A., Zirbel, E. L., & O'Dea, C. P. 1995, ApJ, 451, 88
Blanford, R. D., & Rees, M. J. 1974, MNRAS, 169, 395
Blundell, K. M., Rawlings, S., & Willott, C. J. 1999, AJ, 117, 677
Cavaliere, A., & D'Elia, V. 2002, ApJ, 571, 226
Chiaberge, M., Capetti, A., & Celotti, A. 2000, A&A, 355, 873
Condon, J. J., Cotton, W. D., Greisen, E. W., et al. 1998, AJ, 115, 1693
de Ruiter, H. R., Parma, P., Fanti, C., & Fanti, R. 1990, A&A, 227, 351
Dunlop, J. S., & Peacock, J. A. 1990, MNRAS, 247, 19
Dunlop, J. S., McLure, R. J., Kukula, M., et al. 2003, MNRAS, 340, 1095
Fanaroff, B. L., & Riley, J. M. 1974, MNRAS, 167, 31
Georganopoulos, M., & Kazanas, D. 2003, ApJ, 589, L5
Ghisellini, G., & Celotti, A. 2001, A&A, 379, L1

Giovannini, G., Feretti, L., Gregorini, L., & Parma, P. 1988, A&A, 199, 73
Giovannini, G., Feretti, L., Venturi, T., et al. 1994, ApJ, 435, 116
Giovannini, G., Cotton, W. D., Feretti, L., et al. 2001, ApJ, 552, 508
Gopal-Krishna, Wiita, P. J., & Saripalli, L. 1989, MNRAS, 239, 173
Gopal-Krishna, & Wiita, P. J. 2001, A&A, 373, 100
Govoni, F., Falomo, R., Fasano, G., & Scarpa, R. 2000, A&A, 353, 507
Ishwara-Chandra, C. H., & Saikia, D. J. 1999, MNRAS, 309, 100
Kaiser, C. R., Dennett-Thorpe, J., & Alexander, P. 1997, MNRAS, 292, 723
Komissarov, S. S., & Gubanov, A. G. 1994, A&A, 285, 27
Kormendy, J., & Gebhardt, K. 2001, in The 20th Texas Symposium on Relativistic Astrophysics, ed. H. Martel, & J. C. Wheeler, AIP, 586, 363
Laing, R. A., & Bridle, A. H. 2002, MNRAS, 336, 328
Laing, R. A., & Bridle, A. H. 2002, MNRAS, 336, 1161
Lara, L., Márquez, I., Cotton, W. D., et al. 1999a, A&A, 348, 699
Lara, L., Feretti, L., Giovannini, G., et al. 1999b, ApJ, 513, 197
Lara, L., Cotton, W. D., Feretti, L., et al. 2001a, A&A, 370, 409 (Paper I)
Lara, L., Márquez, I., Cotton, W. D., et al. 2001b, A&A, 378, 826 (Paper II)
Ledlow, M. J., & Owen, F. N. 1996, AJ, 112, 9
Longair, M. S., & Riley, J. M. 1979, MNRAS, 188, 625
Macchetto, F. D. 1999, Ap&SS, 269/270, 269
Machalski, J., Jamrozy, M., & Zola, S. 2001, A&A, 371, 445
Mack, K.-H., Klein, U., O'Dea, C. P., et al. 1998, A&A, 329, 421
McLure, R. J., & Dunlop, J. S. 2001, MNRAS, 327, 199
Morganti, R., Killeen, N. E. B., & Tadhunter, C. N. 1993, MNRAS, 263, 1023
Neeser, M. J., Eales, S. A., Law-Green, J. D., et al. 1995, ApJ, 451, 76
Netzer, H. 1990, in Active Galactic Nuclei, ed. T. J. L. Courvoisier, & M. Mayor (Springer-Verlag), 57
Owen, F. N., & Laing, R. A. 1989, MNRAS, 238, 357
Owsianik, I., & Conway, J. E. 1998, A&A, 337, 69
Peacock, J. A., & Wall, J. V. 1981, MNRAS, 194, 331
Readhead, A. C. S., Xu, W., Pearson, T. J., et al. 1994, A&AS Meeting, 182, 5307
Rees, M. J. 1978, Nature, 275, 516
Scheuer, P. A. G. 1974, MNRAS, 166, 513
Scheuer, P. A. G. 1995, MNRAS, 277, 331
Schoenmakers, A. P., Mack, K.-H., de Bruyn, A. G., et al. 2000a, A&AS, 146, 293
Schoenmakers, A. P., de Bruyn, A. G., Röttgering, H. J. A., et al. 2000b, MNRAS, 315, 371
Schoenmakers, A. P., de Bruyn, A. G., Röttgering, H. J. A., & van der Laan, H. 2001, A&A, 374, 861
Shklovskii, I. S. 1963, SvA, 6, 465
Slee, O. B., Roy, A. L., Murgia, M., et al. 2001, AJ, 122, 1172
Urry, C. M., & Padovani, P. 1995, PASP, 107, 803
Waddington, I., Dunlop, J. S., Peacock, J. A., & Windhorst, R. A. 2001, MNRAS, 328, 882
Wilkinson, P. N., Polatidis, A. G., Readhead, A. C. S., et al. 1994, ApJ, 432, L87
Willott, C. J., Rawlings, S., Blundell, K. M., et al. 2001, MNRAS, 322, 536
Wilson, A. S., & Colbert, A. J. M. 1995, ApJ, 438, 62